

# Carbonization and Geochemical Characteristics of Graphite-Bearing Rocks in the Northern Khanka Terrane, Primorie, Russian Far East

A. I. Khanchuk, L. P. Plyusnina, V. P. Molchanov, and E. I. Medvedev

*Far East Geological Institute, Far East Division, Russian Academy of Sciences, pr. Stoletiya Vladivostoka 159, Vladivostok, 660022 Russia;*

*e-mail: makarovo38@mail.ru*

Received May 4, 2008

**Abstract**—Regional carbonization was examined in Riphean metamorphic complexes in the northern part of the Khanka terrane. The results obtained by various techniques of physicochemical analysis indicate that all petrographic rock varieties of this complex bear elevated concentrations (from  $10^{-4}$  to  $10^{-6}$  wt %) of Au and PGE. XRF data were used to describe a wide spectrum of trace elements: Ti, V, Ni, Cr, Pt, Pd, Re, Rh, Os, Ir, Cu, Hg, Au, Ag, Ta, Nb, Sr, Rb, Zr, La, W, Sn, Pb, and Zn. The Rb/Sr–Ba diagram shows the fields of anatectic granite-gneisses, biotite granites, lamprophyres, graphitized crystalline schists, black shales, skarns, and quartz–graphite metasomatic rocks. The C isotopic composition in graphite from the metagneous rocks (lamprophyres and crystalline schists of the amphibolite facies) corresponds to  $\delta^{13}\text{C}$  from  $-8.5$  to  $-8.7\text{‰}$ , which suggests that the carbon could be of endogenic provenance. The carbon isotopic composition of the greenschist-facies black shales corresponds to  $\delta^{13}\text{C}$  from  $-19.9$  to  $-26.6\text{‰}$ , as is typical of organogenic carbon. The concentrations of precious metals in the rocks are, on average, one order of magnitude lower than in the graphitized crystalline schists. The origin of the precious-metal ore mineralization was likely genetically related to the regional carbonization process.

DOI: 10.1134/S0016702910020011

## OVERVIEW OF THE STUDY AREA

The Khanka terrane contains widespread metamorphic and sedimentary complexes of Proterozoic–Cambrian age, which host, in the northern part of this terrane, a number of broadly known graphite deposits. The Lesozavodsk graphite-bearing district, which was outlined there based on the results of geological survey and exploration, has a total area of 1900 km<sup>2</sup> and includes three cluster of graphite occurrences: Tamga (400 km<sup>2</sup>), Turgenovo (225 km<sup>2</sup>), and Innokent'evskii (100 km<sup>2</sup>) (Fig. 1). Solonenko [1] pointed out that the Ussuri graphite-bearing district is one of the largest graphite-bearing areas in Russia. The whole complex was determined to show traces of early regional metamorphism of the low-gradient broad-zone type to the amphibolite and epidote-amphibolite facies at 730 Ma. The later phase of retrograde metamorphism under conditions ranging from the granulite to greenschist facies was related to collisional events at the Cambrian–Ordovician boundary [2]. Graphite deposits are restricted to zones of intense shearing within a thick collisional belt of folding and normal faulting.

This paper is focused, first of all, on the Turgenovo cluster of graphite occurrences and deposits in the ancient Ruzhinskii diapir. The eroded core of this dome-shaped structure consists of a complicated rock complex of the Ussuri Group, which is metamorphosed to the amphibolite and epidote-amphibolite facies. The complex consists of intercalating garnet–biotite–feldspar and biotite–

quartz–feldspar schists and plagioclase gneisses with marbles and conformable injections of biotite and leucocratic augen granite-gneisses. The marble is skarnified at contacts with granite-gneisses. The unit contains thin (less than 1 m thick) lamprophyre dikes of gabbro-diorite composition with elevated alkalinity, which are conformable with the schistosity of the host rocks. All lithologies were overprinted by graphitization and contain finely divided graphite and its monomineralic veins and lenses. In the schists, graphite is oriented conformably with the schistosity, whereas this mineral in the granite-gneisses and lamprophyres occurs mostly in the form of cutting veinlets and lenses. The carbon concentrations of the rocks vary from fractions of a percent to 39 wt %. The chemical compositions of the aforementioned rock varieties are listed in Table 1. Our study area is unique in that all diverse rock types occurring there are strongly carbonized, up to the development of carbonaceous metasomatites. The strongest graphitization is typical of small granite intrusions cutting across the complex. The carbon source for the magmatic protoliths could be both deep reduced fluids and originally disseminated magmatic carbon. Graphite displays the following relations with minerals of the graphitized granite-gneisses and plagiogneisses: graphite crystallized simultaneously with other minerals and occurs as mutual intergrowths with quartz and biotite. Graphite veinlets may intersect biotite aggregates and, vice versa, biotite veinlets may cut across graphite, and this testifies that the graphite is synmetamorphic.

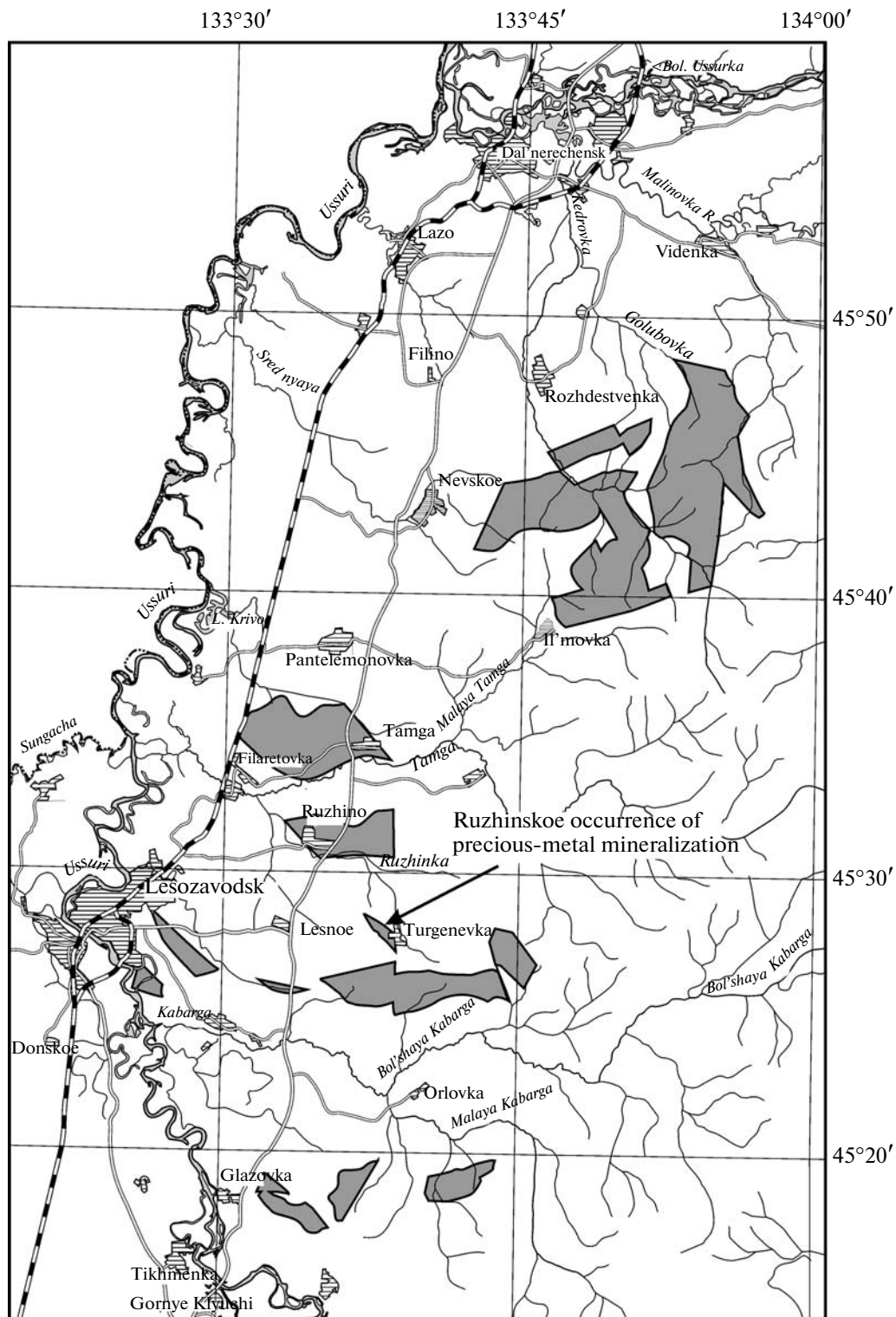


**Fig. 1.** Map of regional graphitization in the northern part of the Khanka terrane. Scale: 1 : 200 000 (based on materials of the Russian Far East Geological Survey).

**Table 1.** Chemical composition (wt %) of rocks from the Ruzhinskii and Tamga deposit.

Oxides	02-3	03-3	04-17	04-40	04-13	04-77*	04-7a	04-101*	02-1	02-4	04-27**	06-14**
	Crystalline schists		Black shales		Skarns		Lamprophyres		Granite-gneisses		Plagiogranites	
SiO <sub>2</sub>	37.74	38.56	81.26	68.30	17.85	34.60	51.30	52.07	70.82	66.50	67.90	67.99
TiO <sub>2</sub>	0.19	0.32	0.42	0.75	0.25	0.38	1.16	1.04	0.22	0.05	0.14	0.09
Al <sub>2</sub> O <sub>3</sub>	12.03	8.95	7.20	12.32	2.48	5.86	21.31	19.29	12.61	12.33	17.27	13.75
Fe <sub>2</sub> O <sub>3</sub>	0.29	2.18	2.20	4.33	0.20	3.17	3.39	7.57	0.58	1.81		
FeO	5.50	0.85	0.34	0.62	2.16	0.35	6.05	1.76	—	—	1.45	4.16
MnO	0.03	0.06	0.01	ñë	0.11	0.05	0.03	0.10	0.02	0.01	0.02	0.12
MgO	0.58	2.16	0.40	0.80	3.01	1.49	1.78	4.01	0.32	0.62	4.90	0.92
CaO	0.20	2.51	0.18	ñë	42.31	20.57	1.95	1.30	3.04	0.28	3.04	4.04
Na <sub>2</sub> O	0.93	1.83	0.47	0.63	0.24	0.59	2.61	2.67	0.95	1.90	2.70	4.35
K <sub>2</sub> O	3.03	1.58	2.20	3.31	0.61	0.99	6.75	7.31	7.90	6.38	1.47	2.38
P <sub>2</sub> O <sub>5</sub>	—	—	0.12	0.23	tr	tr	0.12	0.29	—	—	0.06	n.d.
H <sub>2</sub> O <sup>-</sup>	0.59	tr	0.22	0.10	tr	0.62	0.21	tr	0.10	—	n.d.	n.d.
H <sub>2</sub> O <sup>+</sup>	3.73	5.97	2.11	3.69	1.59	3.63	2.59	1.47	0.98	2.45	n.d.	n.d.
C	36.47	34.57	3.24	4.52	28.81	27.89	0.33	0.77	2.08	7.33	1.70	0.84
Σ	98.11	99.54	100.37	100.37	99.62	100.19	99.92	99.87	99.48	99.58	100.65	98.64

Notes: \* rocks from the Tamga deposit and \*\* rocks from the Ruzhinskii deposit

The complex in question shows no traces of hydrothermal sulfidation, which is typical of most known black-shale complexes. When examined under an optical microscope, the rocks show only rare accessory pyrite and arsenopyrite grains. It is worth mentioning the fault tectonics of the area. Faults and fractures are widespread at the Turgenevo–Tamga group of deposits but are well masked by tectonic graphite-bearing clay, which is graphite mylonite with fragments of graphite–quartz–sericite schists [1].

Recently published data indicate that carbonization processes can be genetically related to precious-metal (PM) mineralization [3]. Because of this, we determined Au and Pt concentrations in samples from the Ruzhinskii deposit, which is located north of the village of Turgenevo, with the rocks exposed in a rubble quarry [4]. The high Au and Pt concentrations determined in these samples stimulated more detailed analytical studies and exploration for Au and PGE. Our research was focused on relations between the graphitization of the rocks and PM mineralization in them and on description of the geochemistry of these graphite-bearing rocks.

#### ANALYTICAL TECHNIQUES USED FOR STUDYING THE PRECIOUS-METAL MINERALIZATION AND THEIR RESULTS

Low PGE concentrations in carbon-bearing rocks and the absence of individual PGE mineral phases in these rocks make it difficult to analyze such rocks for PGE and limit the applicable analytical techniques. The fact that graphitization in rocks of the Khanka terrane affected

significant areas further complicates the solution of this problem because of the high resistance of graphite to oxidative decomposition required for the release of PM. Because of this, rocks in the Ruzhinskii deposit were examined by various techniques of physicochemical analysis.

The first analysis of elevated Au and Pt concentrations in these rocks were made by the physical method of ion mass spectrometry (IMS) at the Institute of Microelectronics and High-Purity Compounds, Russian Academy of Sciences, Chernogolovka, Moscow oblast, with the use of a glow-discharge ionic source at a hollow cathode [5]. The IMS analyses are reported in comparison with the determinations of Au and Pt concentrations in the same samples by ICP on an atom-emission spectrometer and atomic absorption spectrophotometer at the Analytical Center of the Far East Geological Institute, Far East Division, Russian Academy of Sciences, Vladivostok (Table 2). The values obtained by the latter method, which requires time-consuming chemical preparation of the sample, including its decomposition in strongly oxidizing reactants, are notably lower than the IMS method.

In order to confirm relations between the PM mineralization and carbonaceous matter, we analyzed the solution obtained by solving the silicate constituent in aqua regia and HF. These solutions contain all components except graphite, which remains in the residue. The solutions were analyzed on an AA-6200 spectrophotometer and are characterized by low Au concentrations and the absence of Pt and Pd (within the detection limits of the device). The further long-lasting decomposition of the

**Table 2.** Au and Pt concentrations (ppm) in graphite-bearing rocks from the Ruzhinskii deposit

Sample	Au	Pt	Analytical technique*	Rock
02-1	40	n.a.	ICP-AES	Graphite-bearing granite-gneiss
02-3	13	4	IMS	Graphite-bearing granite-gneiss
02-3	30	n.a.	ISP-AES	same
03-1a	5	16	IMS	Granite-gneiss
03-3	3	6.7	IMS	Garnet-biotite-graphite schist
03-5	5	52	IMS	Lamprophyre
04-7a	12	20	IMS	Endoskarn with graphite
04-7a	1.04	1.15	AA	same
04-7b	12	14	IMS	Skarnified marble
04-7b	0.16	1.51	AA	same
04-17	7.2	5	IMS	Sericite-quartz-graphite schist
04-17	0.66	1.30	AA	same
04-29	15	18	IMS	Lamprophyre
04-29	0.46	1.28	AA	same
04-40	17	24	IMS	Sericite-quartz-graphite schist
04-40	0.18	1.29	AA	same
04-9	2.2	3.3	IMS	Black shale, Tamga
04-9	0.14	0.82	AA	same

Note: n.a. means not analyzed; analytical techniques: AA—AA-6200 spectrophotometer, ICP-AES—atomic emission spectroscopy, and IMS—ion mass spectrometer.

graphite residues, which were preliminarily ignited at 600°C, in HClO<sub>4</sub> and HF allowed us to determine their concentrations of Au of up to 16.8 ppm, Pt of up to 14.15 ppm, and Pd of up to 5.67 ppm (Table 3).

Our data indicate that the PM mineralization is closely related to graphite and that much of the metals is lost via

the emission of highly volatile organometallic complexes. Because of this, the “refractive” graphite-bearing rocks were then decomposed by means of oxidizing fluorination, with the use of BrF<sub>3</sub> and KBrF<sub>4</sub>, a technique developed at the Institute of Inorganic Chemistry, Siberian Branch, Russian Academy of Sciences [6]. An advantage of this technique is its selectivity and degree of recovery of the analyzed metals. The analyses of 24 samples from the Ruzhinskii deposit revealed the presence of a broad spectrum of precious metals (concentrations are given in ppm): 0.021–3.57 Au, 0.2–4.41 Ag, 0.04–3.56 Pt, 0.02–0.55 Pd, 0.002–0.055 Ir, 0.011–0.09 Os, 0.007–0.2 Ru, and 0.001–0.74 Rh. Other parts of the same samples were then analyzed for Au by NAA at the Institute of Chemistry, Far East Division, Russian Academy of Sciences. The analyses were carried out with samples 0.5 kg in mass. The results of these analyses are reported, in comparison with the previous ones, in Table 4. Except a few samples, the results in the table are highly consistent (within the accuracy of the methods). However, the maximum Au concentrations in individual samples were detected only by NAA analyses.

The data reported in Tables 2–4 display significant discrepancies between the Au and Pt concentrations of the samples evaluated by various analytical techniques. The greatest analytical errors are caused by the techniques used for the chemical preparation of samples to analysis. Discrepancies between PGE concentrations were detected even between analyses of the same sample [7, 8]. The losses were related to both the release of volatile organometallic complexes [9] and, sometimes, incomplete dissolution of graphite. The “optimal” Au and Pt concentrations were determined by physical methods that do not require any preliminary chemical preparation of the sample. However, IMS analyses of the samples are conducted on small (no greater than 100 mg) portions of solid material, the metal concentrations are overestimated, and this complicated the evaluation of the metal resources and reserves. At the same time, it is expedient to apply this technique in the course of searches of unexposed ore mineralization over large areas with carbon-bearing rocks.

**Table 3.** Concentrations (ppm) of precious metals in samples fractionated into soluble silicates and graphite residue

No.	Au*	Graphite**			ΣAu	Concentration C, (wt %)	Rock
		Au	Pt	Pd			
02/1	0.73	16.68	8.68	5.67	17.41	35	Graphite metasomatite
02/3	0.56	2.83	2.15	0.99	3.39	~4.7	Graphite-bearing plagiogneiss
02/4	0.61	4.18	2.39	1.23	4.79	~6.3	Granite-gneiss
03/1a	—	2.56	4.14	3.31	2.56	5.6	Graphite metasomatite
03/3	0.1	5.37	14.15	7.31	5.47	30	Garnet-biotite-graphite schist
03/5	1.26	0.04	4.46	1.24	1.30	29	Lamprophyre

Note: \* Au concentration in the dissolved constituent was analyzed on an AA-6200 spectrophotometer;

\*\* Au, Pt, and Pd concentrations in graphite ignited at 600°C with the subsequent decomposition and oxidation in HF and HClO<sub>4</sub> (for 30 days).

In generalizing the analytical results on the PM mineralization of the complex in question, it should be mentioned that the highest Au and Pt concentrations were detected in the schists and lamprophyres, with the highest Pt content was only in some found samples of the granite-gneisses and skarns. Pd was found in all samples in average concentrations of 0.02–0.65 ppm; the highest Rh concentrations were identified in the lamprophyres (up to 5.30 ppm), whereas its concentrations in the black shales and granite-gneisses are no higher than 0.01 ppm. For comparison, we considered black shales, granites, and diopside–grossular skarns from the Mitrophanovskaya Group in the vicinity of the Tamga graphite deposit (Table 5), in which the level of Au, Pt, and Pd concentrations ranged from  $10^{-5}$  to  $10^{-6}$  wt %. PM were detected in all lithologies, with the highest concentrations found in the graphitized skarns, a fact attracting attention to these rocks. The examination of crushed samples under an electron microscope revealed gold specks up to 1 mm across, but no individual PGE phases were detected either in the skarns or rocks from the Ruzhinskii deposit in spite of their high Pt contents.

#### GEOCHEMISTRY AND MINERALOGY

The graphitized rocks from the Ruzhinskii deposit, in which the core of a dome structure is exposed, contain a broad spectrum of trace elements (XRF data on 50 samples): Ba, Rb, Sr, Ga, Ta, Nb, Zr, Ti, Cr, V, Ni, Mn, Cu, Zn, Pb, W, La, Re, Pt, Ag, Au, Ru, Rh, and others (Table 6). The highest concentrations of these elements are typical of the lamprophyres, in which the sums of their concentrations (plus those of Hf, Tb, Th, Y, U, and Er, which are absent from other lithologies) reach 1 wt %. Along with these elements, the rocks also contain volatile components: 100–400 ppm F, 40 ppm Cl, and 0.48 wt %  $P_2O_5$ , a fact suggesting the action of transport reactions.

Inasmuch as elevated PGE concentrations were detected in lamprophyre dykes, we attempted to identify the minerals concentrating PGE by examining the samples on a CamScan MV 2300 electron microprobe (beam diameter 157–200 nm) at the Institute of Experimental Mineralogy, Russian Academy of Sciences, Chernogolovka, Moscow oblast. Mineral analyses, which were processed by the INCA Energy 200 computer program, are reported in Table 7 (for sample 03-5). We failed to identify any individual PGE mineral phases. It was, however, found that all of the analyzed magnetite grains contain Pt, and the Pt and REE concentrations of the magnetite are positively correlated, which rules out spurious coincidences. The occurrence of Pt in the magnetite cannot be explained by inclusions of individual Pt minerals at an analytical sensitivity of  $n \times 10^{-4}$  wt %. No Pt was detected in any other phases, including the accessory monazite, thorite, and orthite. Gold is normally contained only in hypersthene. The presence of Pt and Au in the magnetite and hypersthene suggests their magmatic genesis.

**Table 4.** Au concentrations (ppm) in graphite-bearing rocks from the Ruzhinskii deposit: data of neutron activation analysis (NAA) and atomic emission spectroscopy (AES), with preliminary fluoridization decomposition

Sample	NAA	AES	Rock
04-1	≤0.8	0.51	Plagiogneiss
04-1b	1.8	0.71	Graphite veinlet in plagiogneiss
04-2a	≤0.7	0.636	Biotite granite-gneiss
04-3	≤0.2	0.198	Pyroxene skarn
04-3a	≤1.0	0.876	Lamprophyre
04-5	2.6	0.2	same
04-7a	≤1.1	1.18	same
04-13	≤0.3	0.143	Skarnoid
04-16	0.9	1.89	Black shale
04-27	≤1.4	–	Plagiogneiss
04-28	≤0.7	0.23	same
04-29	15.2	1.73	Lamprophyre
04-33	0.4	0.774	Granite-gneiss
04-35	0.4	0.767	Plagiogneiss
04-40	0.4	1.82	Slate
04-68	14.2	n.o.	Graphite metasomatite
04-73	0.8	0.03	Endoskarn
04-74	2.1	0.112	Graphite plagiogneiss
04-75	1.6	–	same
04-77	≤0.5	0.05	Skarnoid
04-78	≤0.4	0.044	Granite-gneiss
04-80	0.9	0.37	Graphite-bearing endoskarn
04-81	1.7	0.043	same
04-101	≤1.2	0.57	Lamprophyre
04-107	6.8	0.29	Marble with up to 7% graphite
04-107k	17.1	0.29	Marble with up to 30% graphite
04-108	0.5	1.01	Vein quartz

Note: NAA analyses were carried out at the Institute of Chemistry, Far East Division, Russian Academy of Sciences (analyst V.V. Ivanenko) and AES analyses were conducted at the Institute of Inorganic Chemistry, Siberian Branch, Russian Academy of Sciences, Novosibirsk (analyst V.N. Mit'kin).

The lamprophyres of gabbro-diorite composition with elevated K and Ti concentrations occur as a suite of relatively thin dikes of variable mineral composition. The rarest varieties are olivine–hypersthene–biotite lamprophyres with garnet and single grains of Cr-bearing spinel (XRD data). These rocks contain the highest Pt concentrations (up to 52 ppm, IMS data) and are noted for high contents of accessory minerals: zircon, apatite, monazite, and magnetite. The pyroxenes commonly contain minor amounts of Ti, V, Cr, and Mn.

The garnet-, hypersthene-, and diopside–biotite lamprophyres have low quartz contents up to 3% but abound in accessory minerals. Another type of the lamprophyres

**Table 5.** Concentrations (wt %) of trace elements in metamorphic rocks from the Ruzhinskii deposit: XRF data

Component	Concentration, wt %		Number of analyses	Rocks
	min	max		
Rh	0.005	0.025	49	lamprophyres, granites, skarns, and black shales
Re	0.00002	0.034	48	same
Os	0.007	0.039	47	same
SrO	0.01	1.30	50	same
Rb <sub>2</sub> O	0.0002	0.12	50	same
NiO	0.0007	0.025	39	same
BaO	0.006	0.61	50	same
La <sub>2</sub> O <sub>3</sub>	0.025	0.048	50	same
Ga <sub>2</sub> O <sub>3</sub>	0.002	0.12	42	same
HfO <sub>2</sub>	0.002	0.015	18	lamprophyres and plagiogneisses
V <sub>2</sub> O <sub>5</sub>	0.001	0.31	35	same
WO <sub>3</sub>	0.003	0.039	5	skarns
MoO <sub>3</sub>	0.03	0.19	4	same
ZnO	0.0001	0.03	14	granite-gneisses and skarns
CeO <sub>2</sub>	0.027	0.094	13	lamprophyres and plagiogneisses
Er <sub>2</sub> O <sub>3</sub>	0.017	0.025	7	skarns and quartz–graphite veins
Tb <sub>4</sub> O <sub>7</sub>	0.002	0.006	5	granite-gneisses
Ir	0.02	0.039	7	lamprophyres and crystalline schists

of diorite composition contains up to 15% quartz, has a diopside–biotite–plagioclase composition, and bears abundant accessory F-apatite, magnetite, pyrite, zircon (with up to 0.40 wt % U, Th, and Hf), orthite (0.80 at % La, 1.76 at % Ce, 0.14 at % Pr, 0.56 at % Nd, and 0.10 at % Sm), F-bearing uranothorite ( $\text{Th}_{0.54}\text{U}_{0.27}\text{Ca}_{0.10}\text{Zr}_{0.06}\text{Y}_{0.02}\text{Si}_{0.99}\text{P}_{0.10}$ , and REE phos-

phates (15.60 at % P, 5.55 at % La, 7.90 at % Ce, 0.54 at % Pr, 1.76 at % Nd, and 0.03 at % U; microprobe data). These lamprophyres have high enough total contents of precious metals. Analyses of the graphitized rocks indicate that all of their varieties always contain Zr, Sr, Ga, La, Ba, Rb, Ni, Ti, V, Cr, Ta, and Nb. Elevated concentrations of Ti, V, Ni, Cr, and Cu are typical of rock complexes in collision zones, in which fluid fluxes transport elements scavenged in lower crustal and upper mantle rocks. The effect of deep-seated basite magmatic chamber is pronounced in the emplacement of lamprophyre dikes of gabbro-diorite composition and the introduction of Ti, Ni, V, Cr, Cu, Pt, PGE, and, perhaps, also Au with deep fluids.

The greatest variations are shown by the concentrations of Ba, Rb, and Sr, which led us to construct Rb/Sr and Rb/Sr–Ba diagrams (Figs. 2, 3). The latter diagram is the most illustrative: it shows clearly distinct fields of the graphitized crystalline schists metamorphosed to the amphibolite facies and black shales of the greenschist facies. The anomalously high Ba concentrations of the black shales reach 4000 ppm. Such concentrations are typical of modern marine sediments and were described in modern diatom oozes from the Aleutian and Mexican trenches [10]. It should be mentioned that the black shales of the Mitrofanovskaya Group are distinguished for high silicon concentrations (up to 81.26 wt %) and are

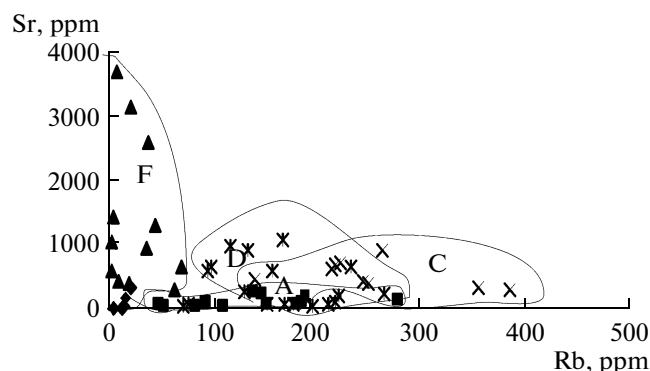


**Fig. 2.** Sr and Rb concentrations (ppm) in rocks from the Ruzhinskii and Tamga deposits: A—crystalline schists and black shales, B—lamprophyres, C—granite-gneisses and granites, and F—skarns and quartz–graphite veins.

dominated by quartz and fine-grained graphite with subordinate amounts of sericite, chlorite, and feldspars. This suggests that the protolith of the rocks consisted of siliceous organic marine oozes. The metamorphism of the latter gave rise to the schistosity of the rocks, the crystallization of sericite, chlorite, and graphite segregations in them, and the development of coarser grained quartz segregations as a result of metamorphic recrystallization.

The gneissose crystalline schists consist of biotite, plagioclase (An<sub>45</sub>), diopside, and garnet and subordinate amounts (<5%) of green hornblende and quartz. The biotite–plagioclase lepidogranoblastic schists consist of plagioclase and quartz and contain biotite and graphite, which accentuate the schistosity of the rocks. In fact, these rocks can be regarded as plagiogneisses (this term is used in Tables 2–4 for brevity). The rocks are unevenly graphitized and contain units rich in graphite and domains of biotite–plagioclase schists practically devoid of this mineral.

The Rb/Sr ratio makes it possible to distinguish between the anatectic gneisses of the Ruzhinskii quarry and Lower Paleozoic alaskite and biotite plagiogranites of the Tamga deposit. The anatectic granite-gneisses have an augen structure with large (up to 1.5 cm) microcline porphyroblasts and more rare garnet of andradite–grossular composition. Their feldspathization and biotitization took place with the participation of granitizing K-rich fluids. The rocks are noted for very low Rb concentrations and strong cataclasis compared to those of the granites. It is worth mentioning that the graphitization of the granite-gneisses is very intense and locally results in carbonaceous metasomatites consisting of predominate graphite and quartz and minor amounts of prehnite and zoisite.

The lamprophyres differ from all other igneous rocks in having elevated Ba concentrations, which are, however, lower than in the black shales. The Ba and K concentrations are positively correlated. Microprobe data indicate that the highest Ba concentrations (up to 1.15 wt %) are contained in biotite.

It is known that Sr is usually contained in carbonates, and the Sr–Rb diagram shows a clearly individualized field of the skarns (with the optimum Sr concentrations), whereas the black shales bear the lowest Sr concentrations, and their field in the diagram overlaps (in terms of Rb concentrations) those of the granite-gneisses and lamprophyres. The Rb/Sr–Ba diagram is, thus, the most suitable for these rocks.

The differences between the geochemical fields (in the Rb/Sr–Ba diagram) of the black shales of the Mitrofanovskaya Group and graphitized schists of the Ussuri Group are confirmed by data on the C isotopic composition of graphite from these rocks. The C isotopic composition of the black shales is characterized by  $\delta^{13}\text{C}$  from  $-19.9$  to  $-26.5\%$  (relative to PDB). These values suggest that the carbon is of organic provenance; such values are typical of sedimentary carbon in Riphean–Early Paleozoic rocks [3]. The schists, granite-gneisses, and lamprophyres contain carbon of homogeneous isotopic composition:  $\delta^{13}\text{C}$  from  $-8.5$  to  $-8.7\%$  (the precision of the

**Table 6.** Au, Pt, and Pd concentrations ( $n \times 10^{-6}$  wt %) in graphitized rocks from the Ruzhinskii and Tamga deposits

Sample	Au	Pt	Pd	Rock
04-6	4.56	8.28	3.21	lamprophyre
04-13	1.30	4.93	10.4	skarn
04-17	17.10	9.03	3.89	black shale
04-18	61.0	11.10	13.40	skarn
04-33	1.93	9.25	1.00	granite-gneiss
04-35	21.20	4.45	18.00	skarn
04-77	7.50	32.10	1.91	skarn
04-80	2.19	23.10	1.24	endoskarn
04-85	6.65	5.46	1.53	marble
04-87	6.44	17.80	1.39	skarn
04-88	2.25	9.21	6.80	granite
04-107	2.16	5.15	2.34	skarn
06-14	2.63	1.15	1.90	granite

Note: Analyses were carried out on a Shimadzu AA-6800 spectrophotometer in electrothermal atomization mode, accuracy:  $2.2 \times 10^{-7}\%$  for Au,  $3.5 \times 10^{-8}$  for Pd, and  $6.9 \times 10^{-7}$  for Pt.

analysis was  $\pm 0.1\%$ ). The high isotopic heterogeneity of the carbon suggests that these rocks do not contain biogenic carbon. Such values characterize carbon of endogenic provenance, and this is confirmed by the abundance of graphite along splay fault and fracture zones at deep faults. A deep endogenic genesis of the carbon also follows from the fact that the graphite contains minute

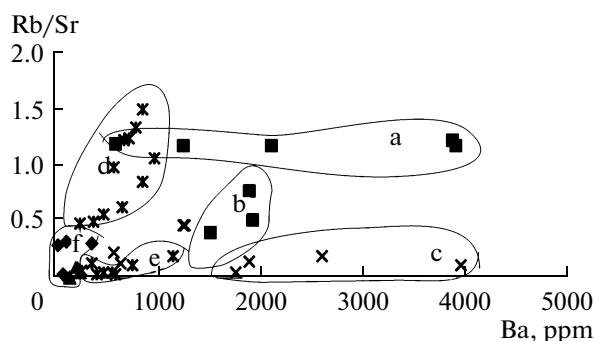


**Fig. 3.** Rb/Sr–Ba diagram (concentrations in ppm) for rocks from the Ruzhinskii and Tamga deposits: a—black shales, b—crystalline schists (plagiogneisses), c—lamprophyres, d—granites from the Tamga deposit, e—granite-gneisses from the Ruzhinskii quarry, and f—skarns and quartz–graphite veins.

**Table 7.** Chemical composition (wt %) of monazite, magnetite, and hypersthene: microprobe data

Element	Monazite	Magnetite	Magnetite	Magnetite	Magnetite	Hypersthene	Hypersthene
Na	0.19	0.14	0.12	0.19	0.33	0.38	0.36
Mg	—	0.24	0.20	0.43	0.36	0.18	0.17
Al	0.48	0.09	0.07	—	—	2.17	2.02
Si	3.87	2.74	2.33	2.68	2.26	19.53	18.07
P	7.29	0.01	0.01	—	—	0.39	0.17
Cl	0.17	0.18	0.16	0.09	0.08	0.36	0.34
K	0.22	0.03	0.03	0.03	0.04	0.13	0.12
Ca	9.14	0.73	0.64	0.53	0.46	3.06	2.84
Ti	0.29	0.05	0.04	0.10	0.09	0.02	0.02
Cr	—	—	—	0.16	0.15	0.15	0.14
Mn	—	0.20	0.19	0.07	0.06	—	—
Fe	5.08	69.97	61.92	69.71	61.37	34.74	32.43
Sr	0.24	0.11	0.10	—	—	—	—
La	3.92	0.35	0.32	0.49	0.44	—	—
Ce	1.55	0.12	0.11	0.27	0.23	0.08	0.17
Pr	0.46	—	—	0.06	0.05	0.32	0.39
Nd	1.20	—	—	0.26	0.24	0.48	0.45
Pt	—	0.09	0.08	0.20	0.17	—	—
Pb	0.24	0.36	0.32	0.26	0.22	0.55	0.51
Au	—	—	—	—	—	0.15	0.13
Th	39.32	—	—	0.20	0.10	0.52	0.48
O	26.35	24.05	32.94	24.05	33.28	36.55	40.99
U	—	—	0.45	—	—	—	—
Total	100.01	99.46	99.58	99.78	99.91	99.76	99.80

globular textures, which were identified in the rocks on a Solver atomic-force scanning microscope (at the Institute of Chemistry, Far East Division, Russian Academy of Sciences) (Fig. 4). The condensation of carbon-bearing gases during their cooling facilitated the development of the globular microtextures as carbon passed from its gaseous to solid state [11].

Graphite from the core of the thermal-dome structure abounds in inclusions of ore and accessory minerals: native Au, magnetite, native Cu, Zn, Bi, Cu–Sn and Cu–Sn–Fe intermetallic compounds, Y–Th–P phases, biotite, pyrite, and arsenopyrite. The electron analysis of the largest spherical gold grain (up to 1 mm across) revealed significant variations in its composition at dis-

crete analytical spots: 100–79.3 at % Au, 0–22.02 at % Ag, and 0–2.2 at % CuO (Fig. 5). The gold grain contains an inclusion of graphite flake, which is also compositionally heterogeneous (at %): 57.92–71.25 C, 0.46–17.40 Au, 28.2–30.0 O, 0.25–2.06 Cl, 0–2.05 K, 0–1.70 Ca, 0–1.70 Si, and 0–1.70 Al. The chemical heterogeneity of the gold and graphite grains and the O and Cl admixtures contained in the graphite testify that these minerals simultaneously crystallized from the gas phase. This conclusion finds support in the occurrence of a nanometer-sized carbon pipe on the gold grain (detected under a high-resolution electron microscope) (Fig. 6). The image shows the transition from the carbonaceous matrix with admixtures of major components to the nanometer-sized pipe of pure

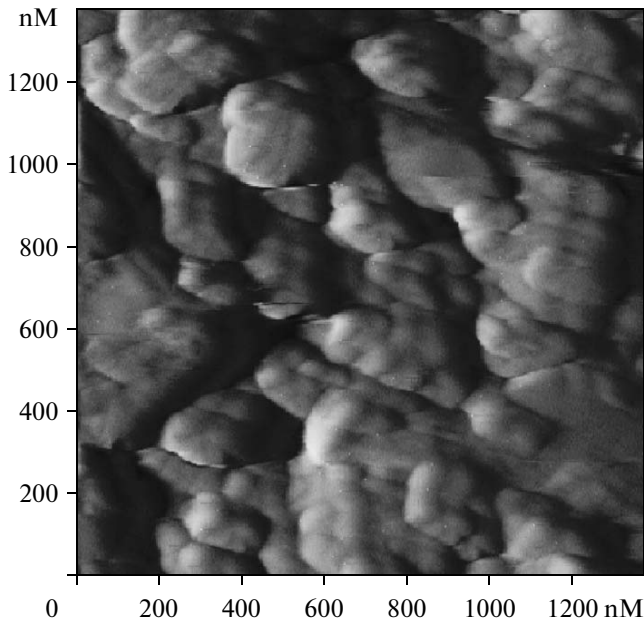


**Fig. 4.** Globular structure of graphite in carbonaceous metasomate developing in granite-gneiss from the Ruzhinskii quarry.

graphite with sharp and clear “geometric” outlines. This is one of the first arguments in support of the occurrence of nanometer-sized carbon pipes in natural gold compounds. The observed coarsening of the gold and graphite crystals resulted from their cumulative recrystallization in the course of regional metamorphism. It is pertinent to mention that the possible sublimation-related genesis of graphite in carbonaceous metasomatites of the Turgenovo deposit was mentioned by Solonenko [1].

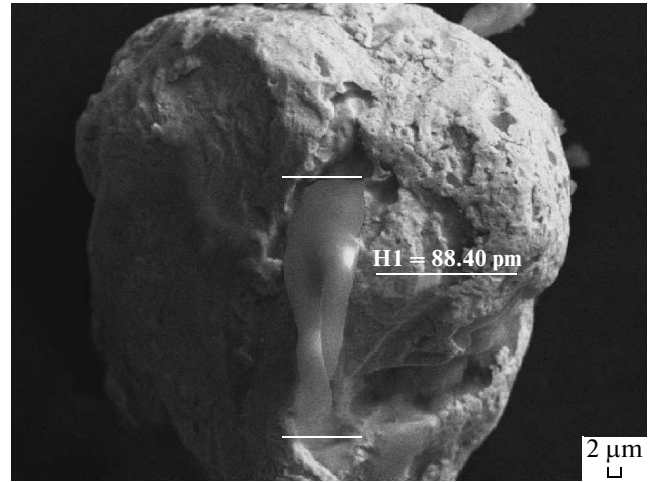


**Fig. 5.** Spheroidal grain of native gold with an inclusion of graphite flake.

The weak character of the oxidation and sulfidization processes and the reduced regime of the gas transport reactions that released carbon and metals in the course of deep degassing were responsible for the absence of individual PGE mineral phases in the rocks. The possibility of metal transport (including that of PGE) during magma degassing was confirmed by data on gas condensates analyzed at Kudryavyi volcano in Iturup Island, Kuriles. The gas condensate definitely contained (ppb) 210 Re, 0.907 Os, 2.4 Au, 0.07 Pt, and 0.009 Ru. The X-ray photoelectron spectroscopy of the sublimates made it possible to additionally identify Pt hydroxyl-complexes and Cl-organic complexes of heavy metals [12].

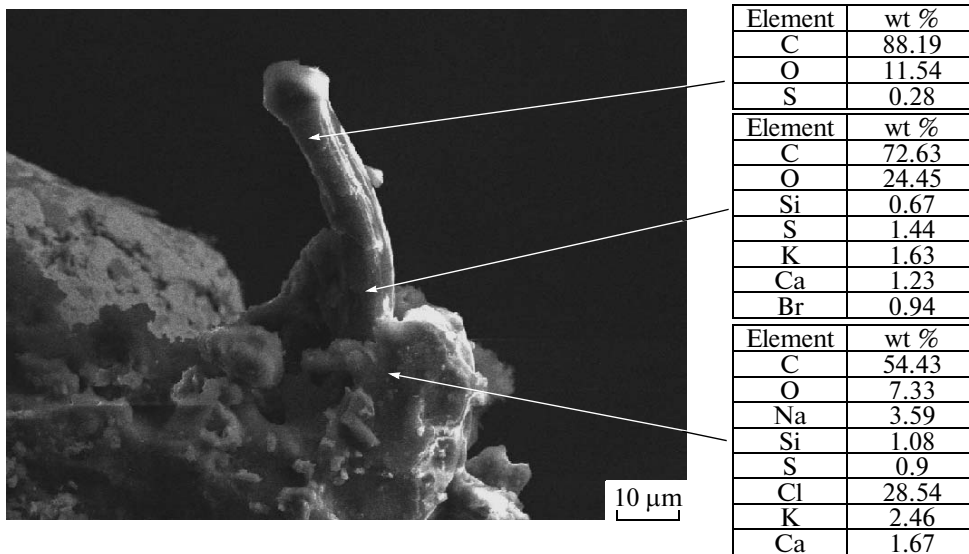


**Fig. 6.** Nanometer-sized carbon pipe on the surface of a gold crystal from skarn, Tamga deposit.

## CONCLUSIONS

Our data indicate that carbon actively participates in ore-forming processes. The rocks in question contain two types of graphite mineralization: evenly disseminated fine-grained graphite and graphite redeposited by high-temperature fluids in shattering and cataclasis zones, with the latter graphite variety forming veinlets, pockets, and monomineralic accumulations. Most researchers believe that carbon is introduced with the gas phases of deep-seated fluids [13]. Some geologists think that black shales provide evidence of periods marked by the catastrophic degassing of the Earth's core [14]. The cooling of ascending high-temperature carbon-bearing fluids stimulates graphite crystallization by the reaction  $\text{CH}_4 + \text{O}_2 = \text{C} + 2\text{H}_2\text{O}$ . The oxidation of hydrocarbons consumes oxygen and, thus, creates highly reduced environments. This process explains widespread inclusions of precious metals, Cu–Sn–Fe intermetallic compounds in graphite, such as those described in the Khanka terrane [7] and elsewhere [15, 16, and others]. The conditions under which native metals and intermetallic compounds were formed in the ores were explained based on the hypothesis of gas-condensation crystallization in a medium of reduced gases of presumably hydrogen–hydrocarbon composition [17]. Hydrocarbon-rich fluids of this type can transport certain ore metals that are contained in the form of organometallic compounds with S, Cl, and other volatile components. The occurrence of Cl in our graphite samples from the Ruzhinskii carbonaceous metasomatites provides further support for this possibility. Zones where carbon-bearing metal transport species are transformed predetermined the geochemical specifics and metallogeny of the host complexes.

Serious problems are faced by researchers studying PGE mineralization without individual PGE minerals in carbonaceous rocks. Anomalously high PGE concentrations found in some graphite-bearing rocks resulted from their interactions with fluxes of deep fluids. Thanks to its chemisorption ability, carbonaceous matter can concentrate metal-bearing fullerenes up to hydrothermal processes of sulfidization and oxidation with the release of PGE in the form of individual mineral phases. Metal-bearing fullerenes are known from experimental data and have unique chemical characteristics: they display very high thermal and chemical resistance at temperatures above 600°C and can easily migrate [18]. One of the interesting morphological features that provide further support for the gas-condensation hypothesis is the ability of native Au, Ag, and other elements to form spheroids and globules as products of the filling of protogas inclusions in a carbonaceous matrix.

The data of Tables 2–6 show that the anomalously high (compared to the Clarke) Au and PGE concentrations were found in all lithologies at the Ruzhinskii and Tamga deposits. This is most likely explained by regional graphitization during the tectonic–magmatic reactivation of the Khanka terrane. The occurrence of graphitization along fault and shattering zones mark zones of tec-

tonic–magmatic reactivation. The ubiquitous traces of graphitization in all lithological varieties of the rocks led us to conclude that the processes of regional graphitization coincided with regional metamorphism related to collisional events at the Cambrian–Ordovician boundary [7].

The ore-hosting complex displays the following features typical of deposits of precious metals in zones of mantle–crustal diapirism: spatial restriction to horst-anticlinal structures, a significant vertical amplitude of the graphite mineralization, occurrence of granitoids of various composition and lamprophyre dikes, elevated concentrations of geochemical different elements in the rocks, and the close association of the precious metals with graphite. These features are typical of ore deposits ascribed to the fluid–magmatic type [18, 19].

The uneven and heterogeneous character of the hypothetical cluster modes of PGE occurrence in graphite makes it difficult to analyze these rocks. In view of this, it is important to develop techniques for the extraction of nanometer-sized Au and PGE grains (much of which is finely divided in the carbonaceous matter) from the rocks.

## ACKNOWLEDGMENTS

We thank G.G. Sikharulidze, V.N. Mit'kin, V.V. Ivanenko, Zh.A. Shcheka, and V.F. Zanina for Au and PGE analyses in rock samples from the Khanka terrane. SEM images of native Au and graphite were obtained by V.G. Kudryavyi (Institute of Chemistry, Far East Division, Russian Academy of Sciences) and P.P. Safonov (Far East Geological Institute, Far East Division, Russian Academy of Sciences).

This study was financially supported by the Presidium of the Far East Division, Russian Academy of Sciences (Grant 06-2-SO-08-029).

## REFERENCES

1. V. P. Solonenko, *Geology of Graphite Deposits of Eastern Siberia and the Soviet Far East* (Izd. Geol. Lit., Moscow, 1951) [in Russian].
2. M. A. Mishkin, A. I. Khanchuk, D. Z. Zhuravlev, and S. I. Lavrik, "First Data on the Sm–Nd Systematics of Metamorphic Rocks in the Khankai Massif, Primor'e Region," *Dokl. Akad. Nauk* **374**, 813–815 (2000) [*Dokl. Earth Sci.* **375**, 1283–1285 (2000)].
3. E. M. Galimov, A. G. Mironov, and S. M. Zhmodik, "Nature of Carbonization in the Carbon-Rich Rocks of the Eastern Sayan," *Geokhimiya*, No. 4, 355–360 (2000) [*Geochem. Int.* **38**, 317–322 (2000)].
4. A. I. Khanchuk, L. P. Plyusnina, and V. P. Molchanov, "The First Data on Gold–Platinoïd Mineralization in Carbonaceous Rocks of the Khanka Massif and Prediction of a Large Noble Metal Deposit in Primorye," *Dokl. Akad. Nauk* **397** (4), 524–529 (2004) [*Dokl. Earth Sci.* **397**, 820–824 (2004)].
5. G. G. Sikharulidze, "Ionic Source with a Hollow Cathode for Element Analysis of Solids," *Mass-Spektrometriya* **1** (1), 21–30 (2004).

6. V. N. Mitkin, A. A. Galizky, and T. M. Korda, "Some Observations on the Determination of Gold and the Platinum-Group Elements in Black Shales," *Geost. Newslet.* **24**, 227–240 (2000).
7. A. I. Khanchuk, L. P. Plyusnina, V. P. Molchanov, and E. I. Medvedev, "Noble Metals in Carbon-Rich Metamorphic Rocks of the Khanka Terrane, Primorie," *Tikhookean. Geol.* **26** (1), 70–80 (2007) [*Russ. J. Pacif. Geol.* **1**, 61–70 (2007)].
8. A. G. Mironov, S. M. Zhmodik, G. M. Kolesov, et al., "Platinum Group Elements in Gold–Sulfide and Base-Metal Ores of the Sayan–Baikal Fold Region and Possible Platinum and Palladium Speciation in Sulfides," *Geol. Rudn. Mestorozhd.* **50** (1), 47–66 (2008) [*Geol. Ore Dep.* **50**, 41–59 (2008)].
9. G. M. Varshall, T. K. Velyukhanova, and A. V. Korochantsev, "Relations between the Sorption Capacity of Carbonaceous Matter with Respect to Noble Metals and Its Structure," *Geokhimiya*, No. 8, 1191–1199 (1995).
10. T. Plank and C. H. Langmuir, "The Chemical Composition of Subducting Sediment and Its Consequences for the Crust and Mantle," *Chem. Geol.* **145**, 325–394 (1998).
11. N. P. Yushkin, A. I. Pavlishin, and A. M. Askhabov, "Ultradispersed State of Mineral Matter and Problems of Nanomineralogy," *Mineral. Zh.* **25** (4), 7–31 (2003).
12. M. A. Yudovskaya, S. Tessalina, V. V. Distler, et al., "Behavior of Highly-Siderophile Elements during Magma Degassing," *Chem. Geol.* **248**, 318–341 (2008).
13. S. M. Zhmodik, A. G. Mironov, L. V. Agafonov, A. S. Zhmodik, et al., "Carbonization of Ultrabasites of Eastern Sayan and Gold–Palladium–Platinum Mineralization," *Geol. Geofiz.* **45** (2), 228–243 (2004).
14. A. A. Marakushev, "Black Shale Formations as an Indicator of Periods of Catastrophic Evolution of the Earth," in *Platinum of Russia* (Moscow, 1999), Vol. 4 [in Russian].
15. F. A. Letnikov, V. B. Savel'eva, Yu. V. Anikina, and M. M. Smagunova, "High-Carbon Tectonites as a New Source of Gold and Platinum," *Dokl. Akad. Nauk* **347** (6), 795–798 (1996) [*Dokl. Earth Sci.* **347**, 509–512 (1996)].
16. Yu. V. Danilova, T. G. Shumilova, and B. S. Danilov, "Forms of Concentration of Ore Elements in Carbon-Rich Metasomatites," *Dokl. Akad. Nauk* **410** (6), 795–798 (2006) [*Dokl. Earth Sci.* **410**, 1263–1266 (2006)].
17. I. D. Ryabchikov and M. I. Novgorodova, "Reducing Fluids in Hydrothermal Ore Formation," *Dokl. Akad. Nauk* **258** (6), 1453–1456 (1981).
18. S. F. Vinokurov, Yu. N. Novikov, and A. V. Usatov, "Fullerenes in the Geochemistry of Endogenic Processes," *Geokhimiya*, No. 9, 937–944 (1997) [*Geochem. Int.* **35**, 822–828 (1997)].
19. P. F. Ivankin and N. I. Nazarova, *Method of Studying Ore-Bearing Structures in Terrigenous Sequences* (Nedra, Moscow, 1988) [in Russian].